Ceramics International 42 (2016) 11150–11160

Contents lists available at ScienceDirect

Ceramics International

journal homepage: www.elsevier.com/locate/ceramint

Factors controlling the mechanical behavior of alumina–magnesia–carbon refractories in air

Vanesa Muñoz, Analía G. Tomba Martinez *

Instituto de Investigaciones en Ciencia y Tecnología de Materiales (INTEMA), CONICET-Facultad de Ingeniería/Universidad Nacional de Mar del Plata, 7600 Mar del Plata, Argentina

ARTICLE INFO

Article history:
Received 3 November 2015
Received in revised form
5 April 2016
Accepted 6 April 2016
Available online 7 April 2016

Keywords:
C. Mechanical properties
D. Al_2O_3
Carbon
MgO
E. Refractories

ABSTRACT

This work analyzes the mechanical behavior of alumina-magnesia-carbon (AMC) refractories in air up to 1260 °C. AMC refractory bricks are used on sidewalls and bottoms working linings of steel-making ladles. In plant, AMC bricks are exposed to air atmosphere during the periods of time when the ladle is empty, such as preheating. Stress–strain relationships were determined in compression, and the following parameters were calculated from these curves: strength, apparent Young's modulus, fracture strain and yield strength. Young's modulus at room temperature was also determined by the impulse excitation technique. To identify the main determining factors, the tested specimens were analyzed by apparent porosity measurements, X-ray diffraction and scanning electron microscopy coupled with X-ray dispersive energy. Thermodynamic simulations of the AMC refractories were also performed using FactSage software, so as to understand the mineralogical changes that occur in the refractories as temperature increases.

© 2016 Elsevier Ltd and Techna Group S.r.l. All rights reserved.

1. Introduction

Alumina-magnesia-carbon (Al_2O_3-MgO-C, AMC) bricks are used mainly on sidewalls and bottoms working linings of steel-making ladles. As structural components, they are exposed to severe mechanical and thermal loading throughout their lifetime, in an aggressive environment comprised of melts (metal and slag), gases and solid particles. Being oxide-C refractories, AMC materials share several features with MgO-C bricks, the most explored member of the family. These features have been reviewed in previous work by the authors [1], but AMC materials also have their own particular characteristics, which require specific research.

Due to carbon-containing refractories' sensitivity to oxidant gases, the study of mechanical behavior is commonly performed in non-oxidizing atmospheres, nitrogen or even a less reactive gas such as argon in order to minimize the loss of the refractory's components (mainly graphite). This has been the case with the few research investigations regarding the mechanical properties of AMC refractories [1–3]. Conversely, this work analyzes the mechanical behavior of three AMC commercial refractories in air. Since the ladle is an open vessel, AMC bricks are exposed to air atmosphere during the periods of time when the ladle is empty, such as preheating, especially in the first campaigns of the ladle (the slag covers the bricks after that). This practice in plant covers the low-middle range of temperature, from room temperature to 1300 °C. Chemical, microstructural and textural changes in AMC bricks begin at temperatures around 300 °C (in particular in the organic binder). The alterations to the composition and microstructure are severe and affect the structural integrity of the bricks.

Stress–strain curves in compression were determined from room temperature to 1260 °C, thus taking advantage of the comprehensive mechanical information they provide. From these curves, the following conventional and nonconventional parameters were calculated: strength, apparent Young's modulus, fracture strain and yield strength. The results obtained by the mechanical evaluation in air were analyzed in comparison with those in a previously reported study performed using a nitrogen flow [1]. Young's modulus at room temperature was also determined using the impulse excitation technique.

Due only to thermal activation, several transformations occur in AMC refractories from 300 °C onwards. The majority of them have been already reported in the literature [4–10]: pyrolisis of resin, graphite and glassy-carbon oxidation, reactions involving aluminum—the most common antioxidant additive used in this type of refractories—which produce Al_4C_3, Al_2O_3 or $MgAl_2O_4$ (MA spinel), and reactions between alumina and magnesia to form MA spinel. These processes are generally accompanied by volumetric and textural changes that result in porosity variations and the

* Corresponding author.
E-mail address: agtomba@fi.mdp.edu.ar (A.G. Tomba Martinez).

http://dx.doi.org/10.1016/j.ceramint.2016.04.021
0272-8842/© 2016 Elsevier Ltd and Techna Group S.r.l. All rights reserved.

formation of microcracks. Not only do these transformations have consequences on the refractory structure at a local or global level, but they also strongly affect the mechanical response of AMC refractories depending on the temperature range at the same time. As can be seen, the situation is rather complex and requires a complete set of experimental techniques to obtain a good description and interpretation of refractory behavior.

To identify the main factors determining the mechanical response of the AMC refractory studied in this paper, the bricks were previously characterized by several methods [9]; then, the mechanically tested specimens were re-analyzed via apparent porosity measurements, X-ray diffraction (XRD) and scanning electron microscopy coupled with energy dispersive spectroscopy (SEM/EDS). Moreover, thermodynamic simulations of the AMC refractories at testing temperatures were also performed using FactSage V.6.4 software, which take into account only their chemical compositions in order to understand the differences in the mineralogical changes occurring in the refractories as temperature increases. The use of this powerful tool in understanding the mechanical behavior of AMC refractories has not been previously reported.

2. Experimental procedure

2.1. Materials

Three Al_2O_3–MgO–C commercial refractory bricks from the same supplier, labeled as AMC1, AMC2 and AMC3, were analyzed. The bricks have differences in the MgO content and the type of raw materials used as sources of alumina.

These refractories were exhaustively characterized using a vast group of analytic techniques: X-ray fluorescence, plasma emission spectroscopy, gravimetry, X-ray diffraction, differential thermal and thermogravimetric analyses, reflection optical microscopy and scanning electron microscopy coupled with X-ray dispersive energy, measurements of density and porosity, Hg-intrusion porosimetry, dilatometric analysis and permanent linear change. The results concerning the characterization of these bricks have been reported previously [9], and the main data are summarized in Table 1.

From these analyses, it was determined that every refractory contains brown fused alumina (EF) plus tabular alumina (TA). AMC1 has a higher proportion of the last type of aggregates with respect to both the EF aggregates and the TA aggregates present in the other two materials. Moreover, it was confirmed that only AMC3 possesses bauxite (with a mullite content estimated around 8–9 wt%), and aluminum is used as an antioxidant in all three materials and in similar proportions. The higher amount of sintered magnesia in AMC2 is distributed in the medium-fine fraction, whereas this component is present only as fine particles in the matrix of AMC1 and AMC3.

Graphite, whose particles have a similar aspect ratio in the three materials, is present at a higher content in AMC2, but its flakes are the smallest. AMC3 has a somewhat lower amount of graphite and its particles are the purest. The bricks contain similar amount of resin as organic binders, although it was not possible to determine what kind of phenolic resin they are (novolaka or resol).

Regarding the texture, AMC2 has a higher amount of open pores, although they are similar in size to those of AMC1. Conversely to what could be expected considering the presence of bauxite as source of alumina in AMC3, which has rather higher porosity (10–15%) than the other two sources of alumina (tabular and fused aluminas, with porosities $<3\%$), this is the brick with the lowest values of open porosity, permeability and pore size. This fact was attributed to a better granulometric fractions packing which would lead to lower levels and sizes of inter-particle pores.

Table 1
Composition and physical properties of AMC refractories.

		AMC1	AMC2	AMC3
Main phases (wt%)	Corundum (Al_2O_3)	82.7 ± 0.3	57.6 ± 0.3	76.6 ± 0.3
	Periclase (MgO)	5.40 ± 0.02	27.0 ± 0.1	6.8 ± 0.1
Secondary phases (wt%)	Graphite (C)	1.7 ± 0.1	3.5 ± 0.1	3.0 ± 0.1
	Resin (C, O, H)	5.4 ± 0.1	5.6 ± 0.1	5.0 ± 0.1
	Aluminium (Al)	1.39 ± 0.02	1.37 ± 0.02	1.60 ± 0.02
Impurities (wt%)	Fe_2O_3, SiO_2, CaO, TiO_2[a]	3.4 ± 0.3	4.9 ± 0.3	6.9 ± 0.3
Global density (Kg/m^3)		3.14 ± 0.02	2.98 ± 0.01	3.14 ± 0.1
Apparent porosity (%)		6.7 ± 0.1	7.8 ± 0.5	4.0 ± 0.1
Total porosity (%)		10 ± 2	12 ± 2	7 ± 2
Permeability ($m^3/Nw/s$)[b]		0.13	0.15	0.08
$\Delta l/l_0^{1260\ °C}$ (%)[c]		1.1	0.8	0.3

[a] Impurities expressed as oxides with contents >0.1 wt%; others impurities are: K_2O, P_2O_5, Cr_2O_3, MnO, ZrO_2, SrO, ZnO.
[b] For ΔP of 3 MPa.
[c] From dilatometric analysis in argon.

The dilatometric analysis of refractories showed that the expansion of AMC3 was less than that of the other two materials. For AMC3, this fact indicates that: a) it has a smaller global thermal expansion coefficient (α), b) the expansive reactions (mainly the formation of spinel) occur at a lower degree and/or c) the microstructure of the material accommodates volumetric changes in a more efficient way due to mechanisms such as, microcracking or the viscous flow of low melting point phases. The presence of Al_2TiO_5 in bauxite aggregates most likely reduces the value of the global α of AMC3. On the other hand, the greater amount of impurities in this refractory would likely promote the formation of low melting point phases, which assist particle-sliding at high temperatures.

3. Mechanical testing

To study the mechanical response of AMC bricks as temperature increases in air (21% v/v de O_2), the measurement of stress–strain curves (s–s) in compression at room temperature (RT), 700, 1000 and 1260 °C, was carried out. The same equipment and experimental conditions used for mechanical testing in a nitrogen atmosphere [1] were used for the mechanical testing in air.

An Instron 8501 (UK) servohydraulic testing machine coupled with a SFL (UK) electric furnace ($MoSi_2$ heating elements) was used. The tests were carried out by displacement control, with a constant rate of 1.67×10^{-3} m/s (0.1 mm/min) up to specimen failure. Cylinders 2.7×10^{-2} m (27 mm) in diameter and 4.0×10^{-2} m (40 mm) in height were used; these were cut from the bricks and their flat faces were machined. The axial displacement of the cylinders was measured with an Instron (UK) capacitive extensometer (± 0.6 μm) for high temperature testing.

Changes occurring in the specimens during the mechanical testing were also analyzed. Fragments of the tested cylinders were measured for apparent porosity, with a methodology based on the DIN 51056 standard [11] using kerosene as the known density fluid and a Sartorius BP 221 S (Germany) analytical balance ($\pm 0.1 \times 10^{-6}$ Kg). Mineralogical analysis of powders ($<70 \times 10^{-6}$ m) obtained by crushing and grinding the tested specimens was carried out by X-ray diffraction (XRD) using a Panalytical X'Pert Pro (The Netherlands) diffractometer, Cu Kα radiation, 40 kV, 40 mA, monocromator, at a rate of 0.0167 °/s. Scanning electron microscopy coupled with X-ray dispersive energy (SEM/EDS) was also performed on the cross surfaces of tested specimens previously stuffed in polyester resin in vacuum,

transversally cut, ground and polished (up to 3 μm diamond paste). A Joel JSM-6460 (USA) microscope was employed. The analysis of the microstructures was carried out only at 1000 and 1260 °C due to the formation of new phases occurring above 1000 °C according to the mineralogical and thermal evolution analyses of these materials [10].

Using stress–strain curves, the following parameters were determined: a) apparent Young's modulus (E_a), calculated as the slope of the linear part of the curve, b) mechanical strength (σ_R), corresponding to the stress value for the maximum load, c) fracture strain (ε_R), which is the strain corresponding to the maximum load and d) yield stress (σ_Y), defined as the stress where the curve deviated from linear behavior. The σ_Y/σ_R ratio in percentage was used as an indicator of the degree of non-linearity of the refractory's mechanical behavior.

Apart from the stress–strain relationship, the Young's modulus (E) was also determined at RT by the impulse excitation technique according to ASTM E1876-09 standard [12]. Using Sonelastic equipment made by ATCP (Brazil) measurements were made twice on prisms of each material ($0.15 \times 0.024 \times 0.025$ m^3) obtained by cutting the bricks. Several measurements were made on each specimen, in bending, longitudinal and torsional modes; from the last mode, the Poisson's ratio (υ) was estimated.

4. Thermal evolution by thermodynamic simulation

The thermodynamic equilibrium phases present in the three AMC refractories at the mechanical testing temperatures in an oxidant atmosphere (oxygen) were calculated using the commercial software FactSage V.6.4. The chemical composition of the refractories were used for the simulation, with the impurities not taken into account. Only the contribution of graphite to the C content was considered since the available databases do not have information regarding resin or the residual carbon coming from its pyrolisis, and the content of the organic binder is similar for the three AMC refractories (Table 1). The compositions considered for each material in the equilibrium calculation are shown in Table 2.

To simulate the oxidant atmosphere in which the mechanical testing was performed (air), a system formed by 0.1 Kg of refractory and 0.003 Kg of gaseous O_2 was selected by taking a rough estimation of the amount of this gas in contact with the specimen in the furnace during the mechanical test. In addition, stoichiometric $MgAl_2O_4$ spinel was selected for the thermodynamic calculation.

5. Results and discussion

5.1. Young's modulus at RT

The values of the Young's modulus at RT obtained by the dynamic method were 43 ± 3 GPa for AMC1, 16 ± 2 GPa for AMC2 and 44 ± 3 GPa for AMC3.

Using one of the most commonly used models to consider the effect of porosity on the Young's, eq. (1) [13,14] as well as the phases rule to calculate the value of E without pores (E_0), Eq. (2), the Young's modulus (E) at RT for AMC refractories was estimated:

$$E = E_0 \exp(-b\pi_a/100) \tag{1}$$

$$E_0 = \Sigma_i \frac{v_i}{V} E_i = \Sigma_i \frac{m_i}{\rho_i} \frac{E_i}{\Sigma_i \frac{m_i}{\rho_i}} \tag{2}$$

In these equations, v_i, m_i, ρ_i and E_i are the volume, the mass, the density and the Young's modulus, respectively, of each component of the AMC bricks (i); b is a constant that depends on the pore shape, and V is the total volume. The following values are used for the calculation: a) the values of E_i for the main phases were taken from those reported in the literature, b) b~4 [15,16] and c) experimental total porosity reported in Table 1. The following values of E were estimated: 235 GPa for AMC1, 186 GPa for AMC2 and 237 GPa for AMC3. The similarity between AMC1 and AMC3 is due to their similar percentages of alumina, the most rigid component of the refractories.

In comparison with experimental data obtained by the excitation method, the values of E calculated from the above equations were quite higher (between five and eleven times higher). This fact has been already pointed out [17], and has been attributed mainly to the presence of microcracks. The effect of this defect on reducing stiffness depends not only on their contribution to the volume of empty space, but also on their amount, size and shape. However, the theoretical fundamentals concerning these effects are not well established, and it is a problem that is far from being solved [17]. In the case of pressed bricks, there is an additional effect related to the orientation of cracks produced by the forming method. In other words, Eq. (2) is based on a microstructural description that only considers the volumetric fraction of phases (one-point correlation function [14]). To describe higher order effects such as size, shape and orientation, higher order functions and other types of techniques for obtaining and analyzing data are required [14].

Microcracks also have an influence on the Poisson's modulus, which decreases with the crack density [17]. The values of this parameter obtained by the impulse excitation technique in torsion mode were determined to be ~0.05 for AMC1 and ~0.11 for AMC3, which are on the order of those reported in the literature for refractory materials [17]. AMC2 exhibited a slightly negative modulus (~ −0.07), which highlights the strong effect of the microcracks' density, which is likely higher in this refractory.

In spite of the difference between the experimentally measured Young's modulus and that estimated by calculation, the relative values were very similar: AMC1 had E values almost equal to AMC3, whereas AMC2 exhibited rather low values. Giving additional support to the idea that the microcracks have a more marked effect in the last refractory, the difference between the measured and calculated Young's moduli was almost twice the magnitude of this difference in the other two materials.

5.2. Mechanical behavior at high temperature

5.2.1. Post-testing characterization and thermodynamic simulation results

Low-magnification images of the microstructure of AMC specimens mechanically tested at 1000 and 1260 °C are present in Figs. 1(a–c) and 2(a–c), respectively. The analyzed surfaces exhibited high deterioration, showing a great amount of the resin used to pack the samples, mainly in AMC2. Distinct characteristics related to the specimen's failure such as microcracks could not be observed in the matrix of the analyzed surfaces. However, some damaged aggregates were detected in post-testing specimens, as shown in Fig. 1 with white arrows, which indicate they played a role in the specimen's failure. Moreover, 'holes' were also

Table 2
Chemical composition of AMC refractories used in the thermodynamic simulation.

	Al_2O_3 (wt%)	MgO (wt%)	Al (wt%)	C (wt%)
AMC1	90.7	5.9	1.5	1.9
AMC2	64.5	30.1	1.5	3.9
AMC3	87.0	7.7	1.8	3.5

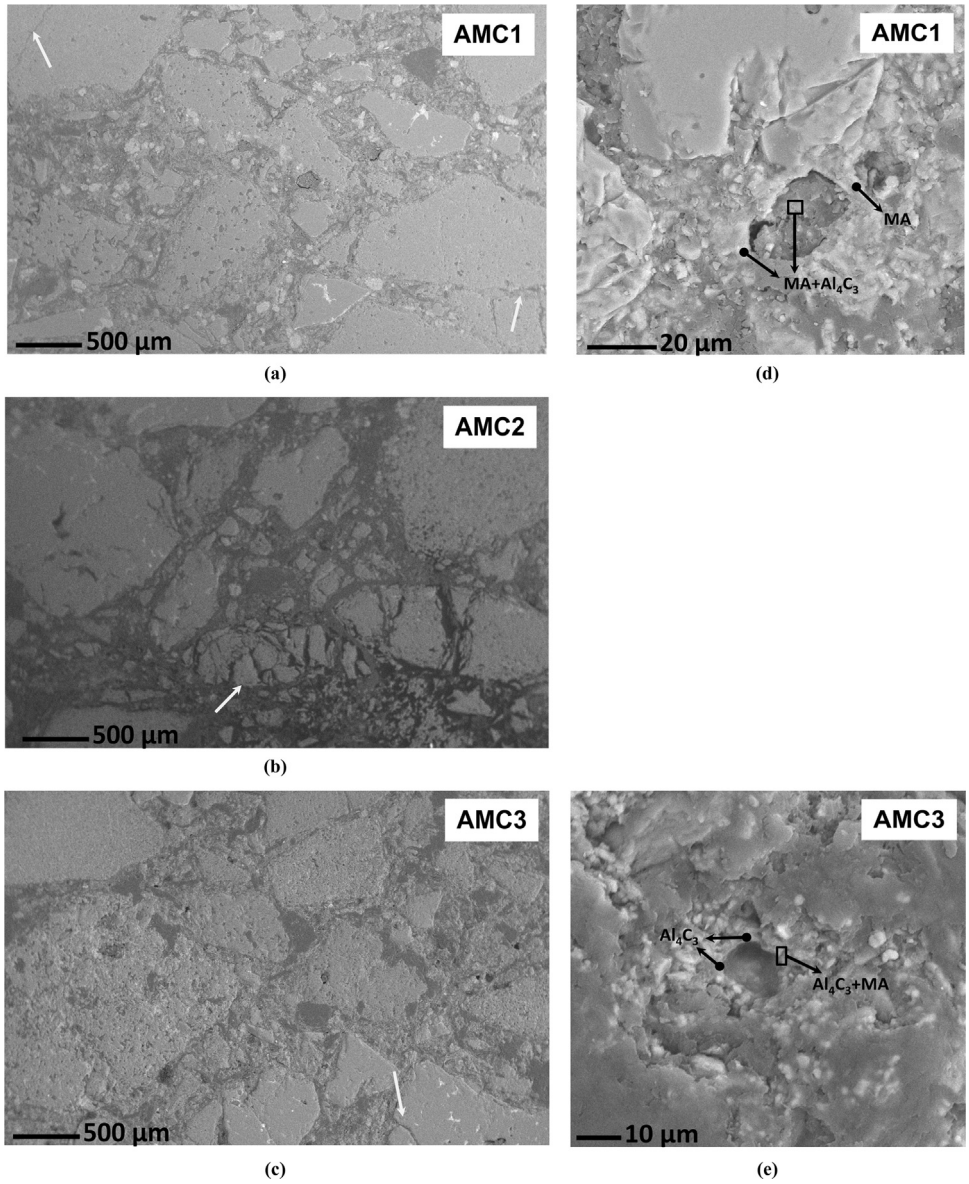

Fig. 1. Microstructure of specimens mechanically tested in air at 1000 °C (SEM/EDS).

distinguish in the matrix of tested cylinders, especially after testing at 1260 °C; this feature is indicated with white narrows in Fig. 2.

Some of the post-testing data for each refractory and testing temperature are reported in Table 3. In this table, the change in the content of some phases involved in the main chemical reactions occurring in AMC refractories up to 1260 °C (determined by XRD and SEM/EDS) are presented, together with the evolution of the apparent porosity (π_a).

With some exceptions, the post-mortem characterization provided results similar to those obtained after the mechanical testing of AMC refractories in nitrogen [1]. The differences were consistent with a combination of a higher oxygen partial pressure in the specimens' environment during the mechanical tests in air and the higher apparent porosities generated in these conditions (the values in N_2 were always $<21\%$ [1]). Both factors tended to increase the amount of O_2 inside the specimens and thus increase the degree to which oxidative process advances, such as with the pyrolisis of resin as well as the glassy-carbon and graphite oxidation. For this reason, the increase in carbon-phase (G) content observed in some samples tested in a nitrogen flow between 700–1000 °C, with respect to the original content, was not detected here. Only the most air-sensitive and porous refractory, AMC2 [9,18], showed an increase in the intensity of the main XRD peak of graphite (26.38°2θ; ICDD File: 41–1487) between 700 and 1000 °C, attributed to the contribution of residual carbon produced by resin pyrolisis, which diffracts similarly to graphite [18]; however, the content remained lower than in the original brick (Table 1). In AMC1, no XRD peaks corresponding to graphite were identified in air at 1260 °C, in contrast with the other refractories.

In spite of the limited information about the fracture process, SEM/EDS analysis gave valuable data about local mineralogical changes occurring during the mechanical tests as shown in high-magnification images of Figs. 1(d and e) and 2 (d–f). Of course, no indications of N-containing phases such as AlN were observed in any of the AMC refractories; in place of this solid, aluminum carbide (AC) was mainly detected around 'holes' (filled with resin), except in AMC2, as observed in Fig. 1d and e; this feature resemble the microstructure typically found as a consequence of the reactions involving metallic aluminum [1,19].

Furthermore, XRD peaks corresponding to MA spinel were more intense in samples tested in air in respect to those that were

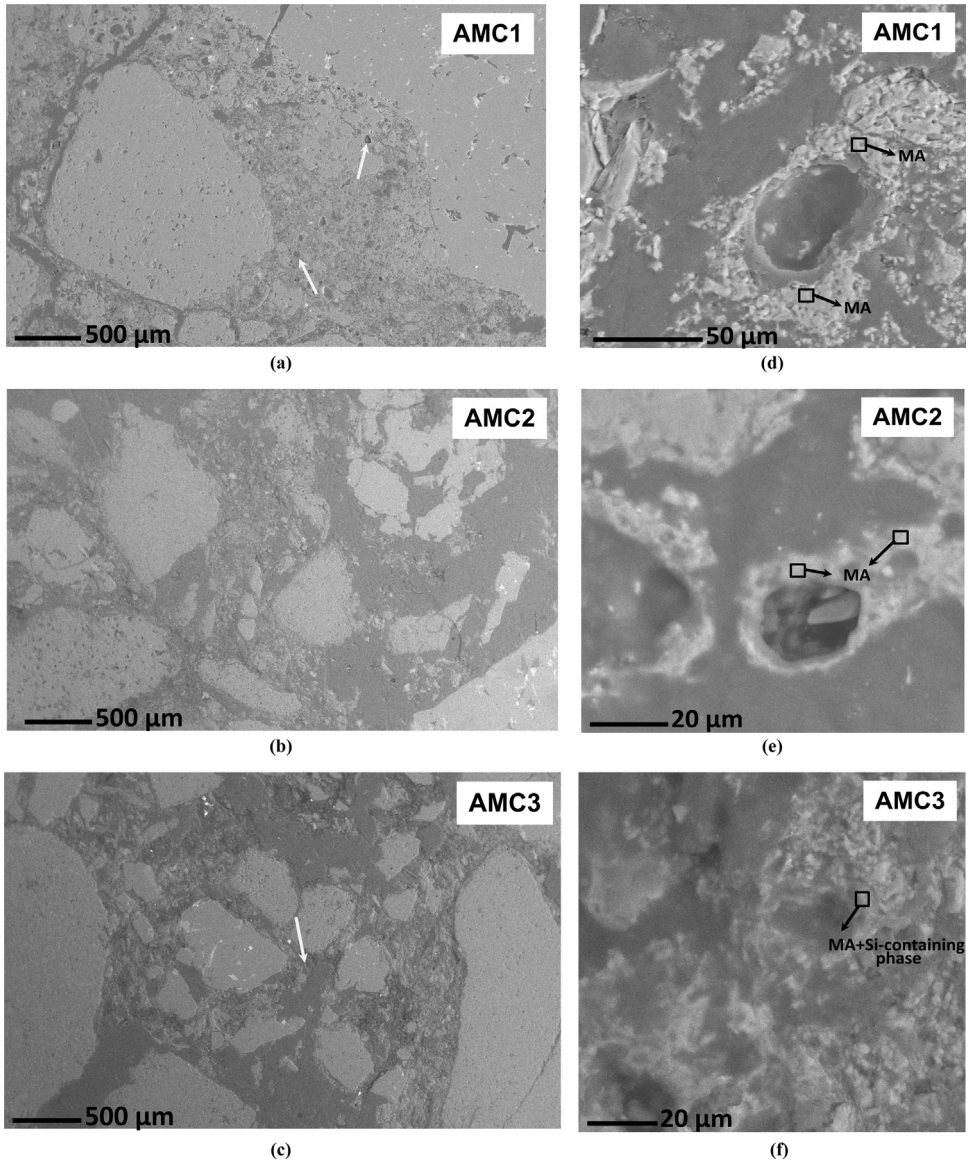

Fig. 2. Microstructure of specimens mechanically tested in air at 1260 °C (SEM/EDS).

Table 3
Mineralogical changes in AMC refractories tested in air (G: graphite, A: aluminum, AC: aluminum carbide, MA: $MgAl_2O_4$ spinel).

		Phases[a] *(by XRD and SEM/EDS)*				π_a *(%)*
		G	A	AC	MA	
AMC1	as-received	xxx	xx	-	-	6.7 ± 0.1
	700 °C	xx	xx	-	-	17 ± 1
	1000 °C	x	x	x	x	21 ± 3
	1260 °C	-	-	x	xx	23 ± 1
AMC2	as-received	xxx	xx	-	-	7.8 ± 0.5
	700 °C	xx	xx	-	-	16.0 ± 0.6
	1000 °C	xxx	x	i[b]	i	23 ± 0.3
	1260 °C	x	-	x	x	27 ± 4
AMC3	as-received	xxx	xx	-	-	4.0 ± 0.1
	700 °C	xxx	xx	-	-	13.0 ± 0.7
	1000 °C	xx	x	x	i	23 ± 3
	1260 °C	xx	-	x	x	21.6 ± 0.7

[a] For the same testing temperature, differences between the content of phases in each AMC bricks have been dismissed.
[b] 'i': used to indicate when analyses were not conclusive.

N_2-tested, which indicates that the reactions producing spinel advanced more in air, where O_2 partial pressure was higher, as was previously reported [5]. Furthermore, according to the SEM/EDS analysis of the specimens reported here, foam-textured spinel, characterized by small grains and pores, was evident as is shown in Figs. 1 and 2. As was previously mentioned, several mechanisms that form $MgAl_2O_4$ spinel also produce fissures and pores [2,5,20–22]. Only few SEM/EDS points located in the peripheral region of the specimens (where the O_2 partial pressure was higher) corresponding to MA spinel composition were identified at 1000 °C, especially in AMC1, whereas this solid phase was clearly present at 1260 °C everywhere. Spinel was mainly identified around or in the vicinity of 'holes', which could indicate that its formation involved MgO and Al or the products of Al reactions (such as Al_4C_3) [19].

As in the nitrogen atmosphere, Si-containing phases were detected in AMC3 specimens mechanically tested at 1000 °C, and particularly at 1260 °C (Fig. 2); taking into account the aspect of the microstructure along with the simultaneous presence of alkaline and earth-alkaline elements, these phases were likely of a glassy nature.

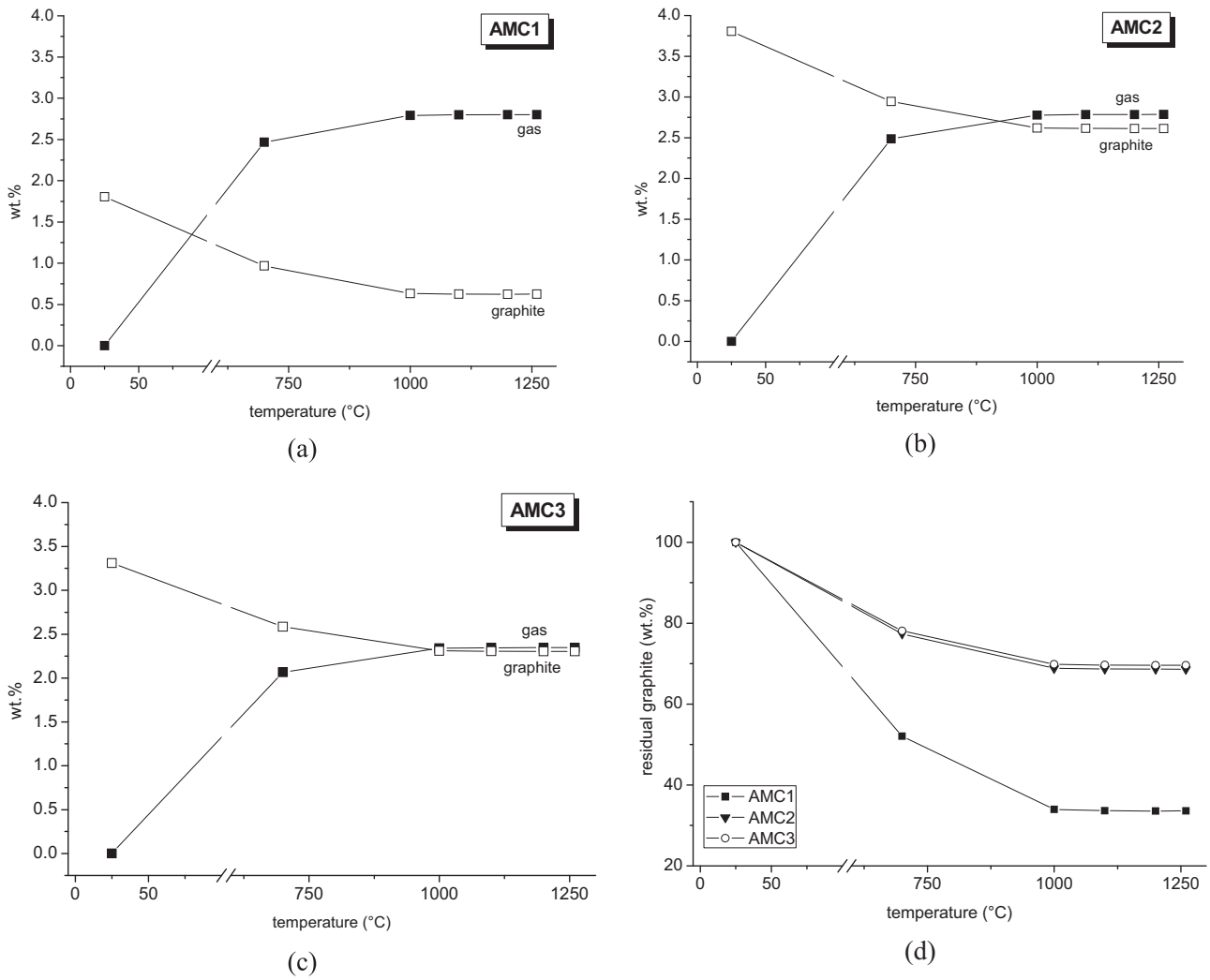

Fig. 3. Variation of gaseous phase (a–c) and graphite (a–d) proportions as a function of temperature for AMC refractories.

Table 4
Solid phase proportions obtained by calculation at 700 and 1260 °C for AMC refractories.

	Al_2O_3 (wt%)		MgO (wt%)		Spinel (wt%)	
	700 °C	1260 °C	700 °C	1260 °C	700 °C	1260 °C
AMC1	76.3	71.7	–	–	20.3	24.9
AMC2	–	–	3.4	3.4	91.2	91.2
AMC3	68.9	62.9	–	–	26.5	32.5

According to thermodynamic simulations, the graphite content shows a significant decrease as the amount of the gaseous phase increases due to the reaction with O_2 (direct oxidation: $C_{(s)}+½ O_{2(g)} \rightarrow CO_{(g)}$), as shown in Fig. 3. However, the rest of solid phases change in a little amount or maintain a constant proportion within the 700–1260 °C temperature range. As for the gaseous phase, which has the same composition in the three AMC materials, it is formed by a mixture of several gases at 700 °C, mainly CO and CO_2 (the latter at a lower proportion). The amount of CO increases at higher temperatures, and it is practically the only component at 1260 °C (> 0.99 of molar fraction). The composition of the solid phase, obtained by calculation for each of AMC refractories at the extreme values of the simulated temperature range (700 and 1260 °C), is reported in Table 4.

The loss of graphite as determined by the thermodynamic simulation is plotted for the three AMC refractories as the testing temperature increase in Fig. 3d. When considering these results, AMC1 loses a greater proportion of graphite in the temperature range of 700–1260 °C, reaching a constant amount at 1000 °C, which represents approximately 35% of the initial content (in weight). Meanwhile, AMC2 and AMC3 show similar behavior, which is attributed to the similar initial graphite content in both materials. They lost a smaller amount of graphite compared to AMC1, retaining a value ~70 wt% at 1000 °C.

A previous paper on the oxidation of these AMC refractories in air [18] showed similar behavior between AMC1 and AMC2, with AMC3 being more chemically resistant to oxidation by air in comparison with the other two materials. Moreover, the data of post-testing specimens reported in Table 3 show that the loss of carbon was complete in AMC1 tested at 1260 °C, although there was still residue of this phase in the other refractories, whose carbon content was reduced with increasing temperature. These results are similar to those obtained by the FactSage simulation, but not entirely. It is worth noting that the equilibrium calculations do not consider the residual carbon produced by resin pyrolisis, which contributed to the carbon content identified as graphite by XRD (Table 3). For the three refractories, the discrepancies between the simulation and the experimental results were attributed to the following principle factors: the oxygen consumed in reactions was constantly renewed by new atmospheric air during the mechanical testing, and the increase in apparent

porosity as the temperature increased allowed a greater amount of gas to enter the specimen. None of these situations was considered in the simulation model.

As for the differences between the AMC materials with respect to graphite loss, the influence of O_2 availability inside the refractories due to the restrictions imposed by the refractories' texture, and the resistance of the graphite flakes themselves (product of their sizes and purity levels, among the main factors) was clear. The difference in the graphite content between AMC1 and AMC3 alone would explain the latter refractory's lower tendency to lose this component (Fig. 3d). Furthermore, the higher resistance manifested by the AMC3 flakes, together with the increased difficulty of gas entering due to the textural characteristics of this refractory (Table 3), would also favor its oxidation resistance during the hot mechanical test in air. Despite the fact that the thermodynamic calculations predict similar graphite losses in AMC2 and AMC3, the higher availability of access channels for gases, together with smaller flakes [9], would favor the oxidation of graphite in AMC2, with its actual behavior similar to that of AMC1.

The thermodynamic simulation calculates that all the magnesia reacts with the Al sources (alumina and metallic aluminum) by 700 °C to form spinel in AMC1 and AMC3 (Table 3), in accordance with their similarly low MgO content. 'Spinel' phase is constitutes mainly, but not only, of $MgAl_2O_4$ (MA); other structures related to the non-stoichiometric character of this solid are also part of spinel. The same occurs in the AMC2 refractory, with an amount of MgO five times greater than in the other two materials, but in this case the proportion of residual MgO and new MA spinel remains constant between 700 and 1260 °C. The comparison of these results with Table 4 those obtained in the post-testing characterization highlights the strong influence of the specimens' texture (porosity) and microstructure (particle and grain size and impurity levels), as will be discussed below.

On one hand, MA spinel was not identified at 700 °C in any of the refractory specimens, but indications of this phase were detected beginning at 1000 °C. Furthermore, this phase was more clearly identified and found in a higher amount in AMC1, in contrast to that established from the equilibrium calculation: according to the thermodynamic simulation, the content of MA spinel in AMC1 should be the lowest. At the other extreme, spinel was clearly detected in the tested AMC2 cylinders upon reaching 1260 °C (similarly to AMC3), whereas the simulation predicts almost the total conversion of MgO in $MgAl_2O_4$ by 700 °C. This fact points out the influence of: a) a smaller size of fine particles of tabular alumina in AMC1, making them more reactive, and b) a lower proportion of periclase forming the AMC2's matrix. For the latter, it was inferred that its higher magnesia content is distributed mainly in the medium-sized fraction, which is why it tends to react less with the Al sources. This factor seems to be more important than the higher reactivity of the aluminum particles, which were finest in this refractory [9].

The thermodynamic calculations predict complete aluminum consumption by 700 °C due to spinel formation, although this component was detected as metal in mechanically tested specimens up to 1000 °C. Even so, aluminum carbide was identified in these samples, which forms due to the reaction of Al with any C source, such as the more reactive residual carbon coming from the resin pyrolisis or the graphite, as has been extensively reported in the literature [20,21,23]. However, Al_4C_3 was not an equilibrium phase under oxidizing conditions, as predicted by the thermodynamic calculation (Table 4). In fact, the formation of solid phases such as Al_4C_3 or Al_4O_4C was predicted by equilibrium calculations performed in absence of gaseous O_2.

The appearance of Al_4C_3 in the tested AMC cylinders indicates that the oxygen partial pressure in the environment of the Al particles was quite lower than that imposed by the external atmosphere. The O_2 partial pressure around the Al particles was primarily defined by the gas entering into the material through the open pores. This process depends on parameters such as the apparent porosity, permeability (related to the interconnection between open pores) and pore size. However, the consumption of oxygen due to reactions with the other refractory components such as graphite has to be considered as well. Furthermore, the advance of O_2 molecules was impeded by the counter-diffusion of products produced by the gaseous reaction, such as CO or CO_2 [18]. In previous paragraphs, it was proposed that the oxygen concentration inside the specimens was higher than that used in the thermodynamic calculation in order to explain discrepancies between the graphite losses simulated and inferred from experimental measurements. Then, the oxidation of graphite and/or residual carbon from resin which consumes O_2 played an important role to reduce the partial pressure of this reactant around Al particles. In this sense, AMC2 is the material having the most available channels of access according to data in Table 1 and the greatest increase in open porosity during high temperature mechanical testing (Table 3). On the other hand, taking into account the tendency to be oxidized of the three AMC refractories [18], a lower proportion of O_2 would be present due to its reaction with graphite in AMC2, the less resistant material to oxidation by air. Since the detection of Al_4C_3 was more difficult in this material at 1000 °C, this might imply that the former factor had a great influence over the mineralogical changes during the mechanical testing of this refractory in air. In AMC1 and AMC3, in which the aluminum carbide was already clearly identified by 1000 °C, the lesser availability of access channels (especially in AMC3) would also have great effect, bearing in mind the higher oxidation resistance of graphite (especially in AMC3).

In summary, the comparison between the results from the equilibrium calculations considering a simple simulation model (based only in the chemical compositions of the main components of the AMC refractories and an estimation of the total amount of oxygen in the external atmosphere) and those of the post-testing characterization showed a strong influence exerted by the texture and the particle sizes of the materials. Furthermore, from this comparison it can be asserted that the chemical transformations were determined by local conditions, which may be different to those imposed by the external atmosphere. Nevertheless some new information about the refractories's characteristics and their incidence on their thermal evolution was obtained from this comparison: a) the effect of a lower particle size of tabular alumina in AMC1 on its tendency to form spinel already at 1000 °C in air, b) the lower proportion of fine magnesia in AMC2 in spite of its high content of MgO, which has a strong influence on spinel formation, and b) the presence of Al_4C_3 and non-reacted metallic aluminum (at 1000 °C) in spite of the external oxidizing atmosphere mainly due to the drop of oxygen partial pressure inside the specimens as a consequence of graphite oxidation, modulated by the access of the gas through the open pores (texture). In future works, the simulation model will be refined in order to reproduce better the actual system in respect to the refractory material and the testing conditions.

5.2.2. Stress–strain behavior

Stress–strain curves in compression give valuable information about the mechanical behavior of the tested refractory (elastic or plastic, linear or non-linear, with softening or hardening) as well as values of its mechanical properties (apparent Young's modulus, strain and strength to fracture) in a range of variable temperatures and atmospheres [24]. These properties can be used to model the mechanical behavior through a constitutive equation. Moreover, they can be analyzed themselves, in order to obtain information

about which are the possible factors determining the material response to mechanical loading (among these factors, those related to the composition, microstructure and texture of refractories are the most interesting, because they can be modified through the brick design in order to enhance the material performance in service). This is the approach used in previous works [20], including that of the authors on the same AMC refractories [1], and it will also be used in the present paper. Unfortunately, since only post-testing analysis can be performed, experimental proofs of such factors' role are often difficult to obtain, in addition to the inherent complexity of this type of refractory, thus only indirect evidence is available.

Before beginning the analysis of the particular characteristics of the mechanical behavior of each AMC refractory in the range of temperatures evaluated here, it is worth clarifying some issues. The E_a parameter defined in this paper, named as '*apparent* Young's modulus', is an indicator of the ability of the material to deform in a reversible as well as irreversible way: the higher the modulus, the greater the stiffness and less deformable the material. The graphite (by sliding along the basal planes and the crumbling of flakes), pores (which contribute with a null Young's modulus) and microcracks of any origin [1] (by their propagation) are considered to be mainly responsible for the capacity of this type of refractory to deform. These same factors are which cause the deviation from linear behavior and the softening observed in the stress–strain curves. The microcracking is considered the factor that determines the softening behavior: the coarse- to medium-sized particles act as obstacles in the extension of microcracks that run easier through the bonding phase due to its low cohesion.

On the other hand, mechanical strength is related to the type and/or the size of the flaws limiting the load bearing capacity of the refractory structure, in combination with the mechanical strength of the main components of the structure. In these refractories, flaws are commonly the discontinuities between the matrix-aggregates interfaces, and the microcracks and pores present in the bonding phase. However, despite the fact that fracture occurred preferably through the matrix, the cross surfaces of the specimens show some broken aggregates (Figs. 1 and 2). Based on this fact, it is expected that finest particles, which are less resistant, are also involved in the material's failure.

Typical stress–strain curves of each AMC refractory at different testing temperatures are shown in Fig. 4. In Figs. 5 and 6, mechanical parameters vs. testing temperature are plotted for the three AMC materials. Lines are used to connect the media values for clarity only and do not indicate the change in the respective parameter with temperature.

The values of E_a (apparent Young's modulus) obtained from the stress–strain curves (quasi-static method) at room temperature were lower than the Young's modulus determined by the dynamic technique, as has been previously discussed [17]. Besides differences in the thermodynamic aspects of the two types of techniques (the dynamic method is an adiabatic measurement whereas the quasi-static method is an isothermal one; thus, the Young's modulus obtained from the former is higher), anelastic and even irreversible deformation [25,26], such as the sliding of graphite flakes or microcracking, add to the elastic strain in the case of oxide-C refractories. The presence of additional deformation mechanisms and the effects of accommodating the specimen in the load application system are also reasons why the elastic parameter derived from the stress–strain curves was also lower than that predicted from Eqs. (1) and (2). For the analyzed AMC refractories, the elastic parameters obtained from stress–strain curves represented between 20% and 60% of the values measured with the impulse excitation technique; these differences are similar to or lower than those reported by Bradt for other types of refractories [17]. AMC2 exhibited the smallest difference between these experimental values, which could suggest that microcracks relevantly affect both measurements in a similar way.

In general, the stress–strain curves determined in the air atmosphere were rather similar to those obtained in the nitrogen flow, and the factors determining high-temperature mechanical behavior were also similar to those previously discussed [1]: a) the presence of graphite, which results in a greater ability to deform (flexibility), b) the formation of new solid phases (aluminum carbide and MA spinel) at a local level that help consolidate the structure but could also contribute to porosity (the formation of spinel, for instance), and c) the formation and extension of microcracks (considered the primary cause of the softening behavior) and changes in porosity. For this reason, only the main differences between the mechanical responses at high temperature under both the nitrogen flow and air atmospheres will be discussed. Differences in the specific parameters values between AMC1, AMC2 and AMC3 which are related to their composition, microstructure and texture, and their alteration with temperature, have been previously discussed and will not be dealt with here in detail.

After the expected drop in mechanical performance between RT and 700 °C, recovery of the main parameters, such as σ_R and E_a, was also observed at 1000 °C in air. However, unlike what occurred with N_2, the apparent Young's modulus of AMC3 was so higher that exceeded the value at RT. The decreased ability to deform (also observed in the fracture strain values, Fig. 6a) and the subsequent increase of E_a was mainly due to the oxidation of graphite. The contribution of this process, together with the incipient formation of the new phases detected at 1000 °C, exceeded the contrary effect of porosity growth (Table 3) on the apparent Young's modulus. The reason why E_a of AMC3 increased so much in air was the higher amount of graphite lost by oxidation (which occurred upon reaching 1000 °C for this material) in this atmosphere than in N_2 flow. As was previously reported [18], AMC3 exhibited the strongest drop of the graphite amount between 700 and 1000 °C in air, whereas this happened between RT and 700 °C in AMC1 and AMC2. In these two materials, the growth of porosity, on one side, and graphite loss and new solid phase formation on the other (especially in AMC1), could offset each other, leading to the smaller variation of E_a between 700 and 1000 °C, similar in air and nitrogen.

Moreover, the deviation from linear behavior occurred before in AMC3 when compared with testing at 700 °C (lower σ_Y/σ_R, see Fig. 6b), which was unexpected considering the contribution of the analyzed factors. AMC3 showed a certain ability to accommodate volumetric changes, with microcracking being one of the possible causes for this (see Section 1.Materials). Thus, the more pronounced non-linearity of this material at 1000 °C could be associated with a greater contribution of microcracking.

One notable difference regarding the stress–strain behavior of AMC refractories in air was the general decay in mechanical performance at 1260 °C when compared with the other testing temperatures, in contrast to that observed when nitrogen was the testing atmosphere, especially in AMC1. The decrease in σ_R for this refractory was attributed to the increase in porosity and microcracks, which could not be counterbalanced by the binding effect of the new formed phases (Al_4C_3 and MA), even though these chemical reactions progressed the most. According to Baudín et al. [19], the formation of aluminum carbide could produce microcracks as well as the crystallization of spinel [19,20]. In addition, the texture of the spinel observed by SEM involving pores could also be the cause of poor cohesion. Furthermore, the absence of carbon phases in AMC1 in this testing condition (see Table 3) implies that the C–C network left by the resin pyrolisis, which contributed to structural cohesion at 1000 °C, was completely lost. Taking into account fracture strain, microcracking exerted a greater influence than the absence of graphite in AMC1; as a

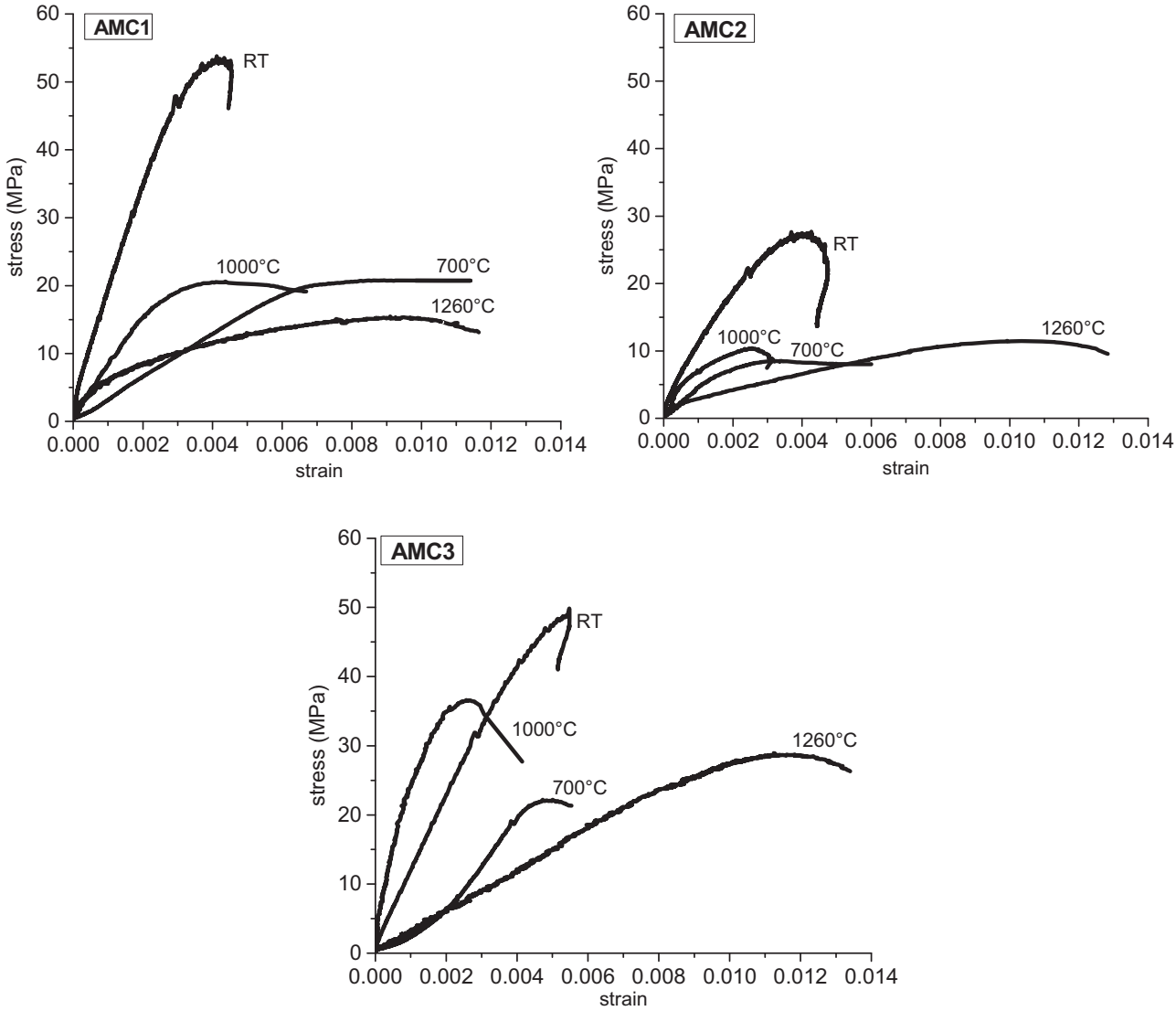

Fig. 4. Typical stress–strain curves of AMC refractories at different testing temperatures.

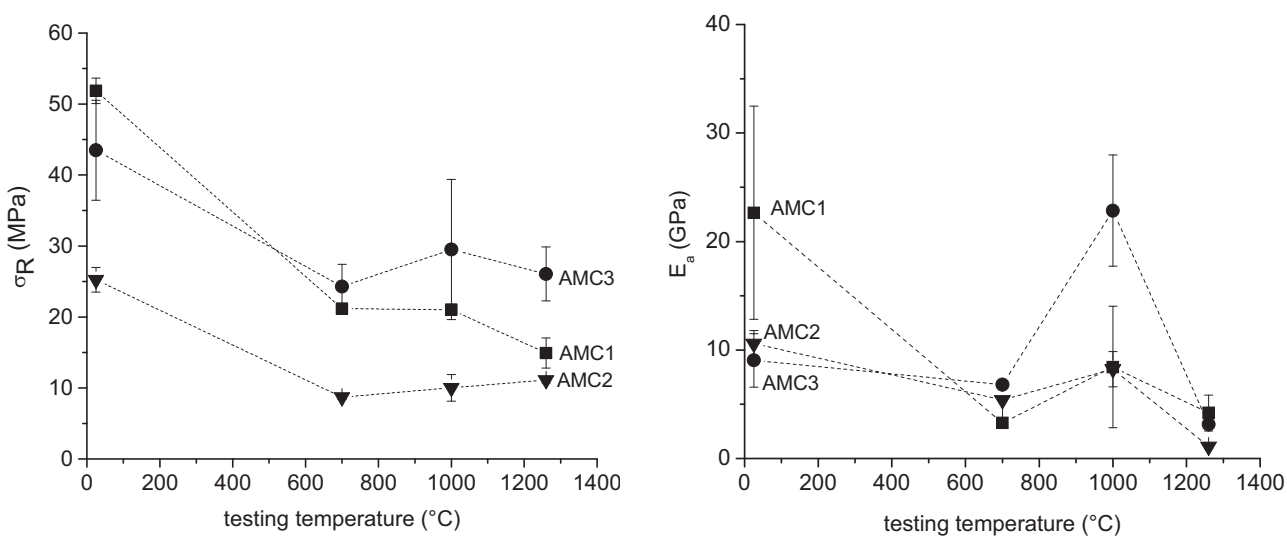

Fig. 5. Variation in the mechanical strength (σ_R) and the apparent Young's modulus (E_a) of AMC refractories with the testing temperature.

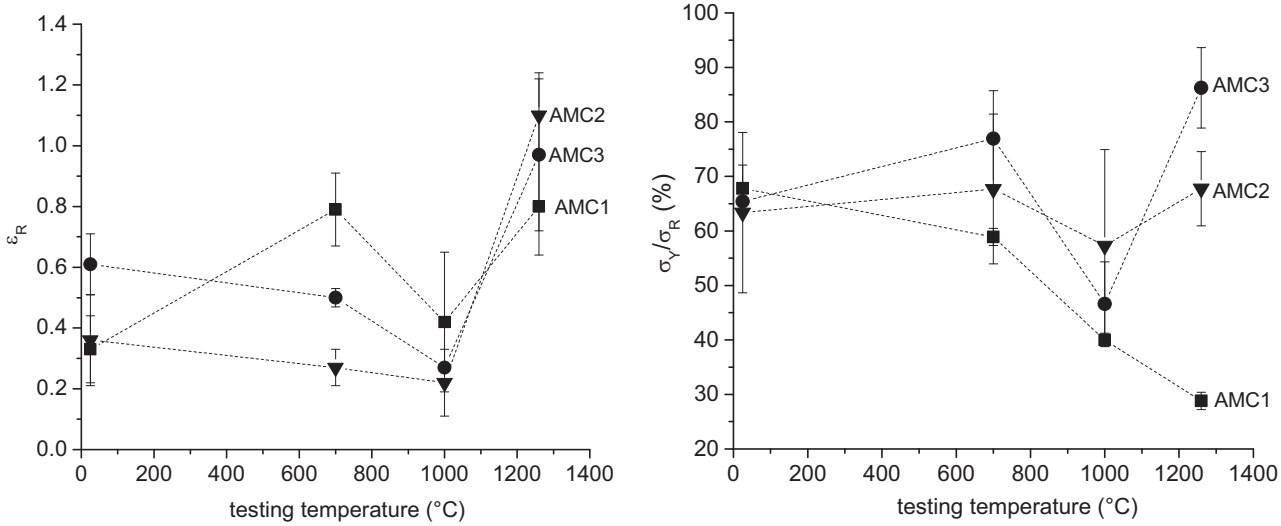

Fig. 6. Variation in fracture strain (ε_R) and the σ_Y/σ_R percentage ratio of AMC refractories with testing temperature.

consequence, the degree of non-linearity increased from 1000 to 1260 °C (but not the apparent Young's modulus, which remained unchanged for this material).

Meanwhile, AMC2 and AMC3 exhibited similar behavior in both air and nitrogen in terms of the variation in mechanical strength between 1000 and 1260 °C, partially because the carbon phases were not completely lost. However, in contrast to previous results in N_2, a significant increase in fracture strain was observed (also for AMC1), which resulted in a significant reduction in E_a between 1000 and 1260 °C. A greater ability to deform at 1260 °C was attributed to the following determining factors: high porosity (greater than in the N_2 atmosphere) and microcracking (favored by the same processes mentioned for AMC1) in AMC2, and the presence of Si-containing glassy phases, which have viscoplastic behavior [1,25], in AMC3. Moreover, the presence of carbon phases in both refractories still contributed to the deformation mechanisms and, similar to what happened in AMC1, the binding effect expected from the formation of new solid phases did not prevail in air at 1260 °C. This could be due to the local character of these new solids or the low capacity for providing a rigid structure. The mechanical behavior was also more linear at 1260 °C (higher σ_Y/σ_R), particularly for AMC3, confirming that microcracking contributed less than the viscous phases, as was previously discussed [1].

The distinct mechanical behavior exhibited in air when compared to the nitrogen flow reveals the significant effect of the O_2 partial pressure generated inside the specimen. This parameter not only accelerated the oxidative process (oxidation of graphite and pyrolisis of resin) directly, but also determined the final products and the rate of reaction between the components themselves within the AMC refractories (formation and decomposition of carbides, or oxicarbides, and spinel formation), which affected porosity indirectly. For this reason, the oxygen concentration strongly influenced the competing factors that determined the stress–strain response and the mechanical parameters.

Furthermore, when considering the mechanical performance of AMC refractory bricks in air, AMC1 and AMC3 were the most resistant materials in the whole range of tested temperatures, as was observed in the non-oxidant atmosphere. However, the relative order of both materials changed as testing temperature increased: while AMC1 exhibited the highest mechanical strength at RT, AMC3 had the highest load-bearing capacity at 1260 °C (only in air) even though it has the lowest quality of alumina raw material (bauxite) and the highest impurity levels, which generated viscous phases. The behavior shown by AMC3 was partially attributed to its lower apparent porosity, which kept constant between 1000 and 1260 °C in air, in contrast to AMC1, where this parameter increased significantly in the same temperature range. Regarding the materials' stiffness, the AMC refractories studied tended to become more similar as the testing temperature increased, except for AMC3 at 1000 °C, which was rather rigid due to the oxidation of graphite that was detected at this temperature (due to its low permeability and the higher oxidation resistance of its flakes). As occurred in the N_2-flow, AMC2 displayed poor behavior, although the combination of low stiffness and low mechanical strength could be favorable in reducing the tendency of crack propagation by thermal shock.

6. Conclusions

The mechanical behavior of commercial AMC refractories at temperatures < 1300 °C under air has been studied with the help of several experimental and simulation tools: a comprehensive characterization of the original materials, stress–strain tests in compression, post-testing characterization and equilibrium calculations. This combination of techniques has not been previously reported when researching the mechanical performance of this type of complex material, and it allows us to identify the main factors that may determine the material's behavior in the low-middle temperature range.

The relevance of the local partial pressure of oxygen (which is different from that of the external atmosphere) on mineralogical changes during high-temperature mechanical testing was pointed out. The most important thermally activated processes that exerted influence on the mechanical properties in air were the pyrolisis of resin, the oxidation of carbon phases and textural changes (porosity and microcracks). Despite new solid phases such as Al_4C_3 and $MgAl_2O_4$ spinel crystallizing beginning at 1000 °C, they did not play a significant role in the cohesion of the refractories' structure up to 1260 °C.

The main differences observed in the mechanical response of AMC refractory bricks in both non-oxidizing (nitrogen flow) and oxidizing (air) atmospheres were detected at the highest temperatures, 1000 and 1260 °C. For the last temperature in particular, the general performance of the materials decayed in air, in contrast to what occurred in N_2-testing. AMC1 and AMC3 also performed better mechanically in air, but AMC3 showed the highest mechanical strength at 1260 °C.

Acknowledgements

This work was supported by the Agencia Nacional de Promoción Científica y Tecnológica (ANPCyT) of Argentina under Project "Degradación termoquímica y termomecánica de refractarios óxido-C de uso siderúrgico" (PICT2006 N° 1887). The authors also thank to Dr. E. Brandaleze for the possibility of using the FactSage software.

References

[1] V. Muñoz, A.G. Tomba Martinez, Thermomechanical behaviour of Al_2O_3–MgO–C refractories under non-oxidizing atmosphere, Ceram. Int. 41 (3) (2015) 3438–3448.
[2] A. Watanabe, H. Takahashi, S. Takanaga, N. Goto, O. Matsuura, S. Yoshida, Thermal and mechanical properties of Al_2O_3–MgO–C bricks, Taikabutsu Overseas 10 (1990) 137–147.
[3] L. Musante, V. Muñoz, M.H. Labadie, A.G. Tomba Martinez, High temperature mechanical behavior of Al_2O_3-MgO-C refractories for steelmaking use, Ceram. Int. 37 (5) (2011) 1473–1483.
[4] Y. Sasajima, T. Yoshida, S. Hayama, Effect of composition and magnesia particle size in alumina-magnesia-carbon refractories, in: Proceedings of the Unified International Technical Conference on Refractories UNITECR'89 (Anaheim, CA), 1989, pp. 586–603.
[5] P. Williams, A. Hagni, Mineralogical studies of alumina magnesia carbon steel ladle refractories, in: Proceedings of the Unified International Technical Conference on Refractories UNITECR'97 (New Orleans, LA), 1997, pp. 183–192.
[6] A.D. Gupta, K. Vickram, Development of resin-bonded alumina–magnesia–carbon bricks for steel ladle applications, Interceram 48 (5) (1999) 307–310.
[7] S.K. Nandy, P.K. Choudhury, D.P. Chakraborti, Resin-bonded Al_2O_3–MgO–C brick for steel ladle, Am. Ceram. Soc. Bull. 79 (7) (2000) 67–70.
[8] J. Pötschke, T. Deinet, G. Routschka, R. Simmat, Properties and corrosion of AMC-refractories. Part I: Characterisation and oxidation; in: Proceedings of the Unified International Technical Conference on Refractories UNITECR'03, Osaka, Japan, 2003, pp. 580–583.
[9] V. Muñoz, P. Pena, A.G. Tomba Martinez, Physical, chemical and thermal characterization of alumina-magnesia-carbon refractories, Ceram. Int. 40 (7) (2014) 9133–9149.
[10] V. Muñoz, A.G. Tomba Martinez, Thermal evolution of Al_2O_3–MgO–C refractories, Procedia Mater. Sci. 1 (2012) 410–417, http://dx.doi.org/10.1016/j.mspro.2012.06.055.
[11] DIN EN 993-1 (DIN 51056). Method of test for dense shaped refractory products. Determination of bulk density, apparent porosity and true porosity, 1995.
[12] ASTM E1876-09. Standard Test Method for Dynamic Young's Modulus, Shear Modulus, and Poisson's Ratio by Impulse Excitation of Vibration, 2009.
[13] J.B. Wachtman, Mechanical properties of ceramics, Wiley-Interscience, USA, 2009.
[14] W. Pabst, E. Gregorová, G. Tichá, Elasticity of porous ceramics – A critical study of modulus-porosity relations, J. Eur. Ceram. Soc. 26 (7) (2006) 1085–1097.
[15] R.L. Coble, W.D. Kingery, Effect of porosity on physical properties of sintered alumina, J. Am. Ceram. Soc. 39 (11) (1956) 377–385.
[16] T. Zhang, H. Hübner, J.A. Rodrigues, V.C. Pandolfelli, Effect of hydratable alumina binder on the creep behavior of cement-free high-alumina refractory castables, in: Proceedings of the Unified International Technical Conference on Refractories UNITECR'97, New Orleans, LA, 1997, pp. 1337–1346.
[17] R.C. Bradt, Elastic properties of refractories: their role in characterization, Refractories Application & News, May/June 2007, 11-26.
[18] V. Muñoz, P.G. Galliano, E. Brandaleze, A.G. Tomba Martinez, Chemical wear of commercial Al_2O_3–MgO–C bricks by air and basic slag, J. Eur. Ceram. Soc. 35 (5) (2014) 1621–1635.
[19] S. Zhang, N.J. Marriot, W.E. Lee, Thermochemistry and microstructures of MgO–C refractories containing various antioxidants, J. Eur. Ceram. Soc. 21 (2001) 1037–1047.
[20] C. Baudín, C. Alvarez, R.E. Moore, Influence of chemical reactions in magnesia–graphite refractories I, Effects on texture and high temperature mechanical properties, J. Am. Ceram. Soc. 82 (12) (1999) 3529–3538.
[21] C. Baudín, High temperature mechanical behavior of magnesia-graphite refractories, in: J. Bennett, J.D. Smith (Eds.), Ceramic Transactions, Fundamentals of Refractory Technology, 125, American Ceramic Society, Westerville, OH, 2001, pp. 73–92.
[22] Y. Kiyota, Reduction of permanent linear change of Al_2O_3–MgO castable, in: Proceedings of the Unified International Technical Conference on Refractories UNITECR'07, Dresden, Germany, 2007, pp. 546–549.
[23] C. Taffin, J. Poirier, The behaviour of metal additives in MgO–C and Al_2O_3–C refractories, Interceram 43 (5) (1994) 354–358 / 458-460 [6].
[24] V. Muñoz, G.A. Rohr, A.L. Cavalieri, A.G. Tomba Martinez, Experimental methodology of the mechanical evaluation of oxide-carbon refractories by strain measurement, J. Test. Eval. 40 (1) (2012).
[25] J.M. Robin, Y. Berthaud, N. Schmitt, J. Poirier, D. Themines, Thermomechanical behaviour of magnesia-carbon refractories, Brit. Ceram. Trans. 97 (1998) 1–10.
[26] N. Schmitt, Y. Berthaud, J. Poirier, Tensile behaviour of magnesia carbon refractories, J. Eur. Ceram. Soc. 20 (12) (2000) 2239–2248.